

## Chapter 4

### Contrasting Drug-Receptor Interactions at Neuronal vs. Muscle-Type Nicotinic Acetylcholine Receptors: The Neuronal $\alpha 4\beta 4$ Receptor\*

*\*This chapter is adapted in part from: Puskar, N. L.; Xiu, X.; Lester, H. A.; Dougherty, D. A. Two neuronal nicotinic acetylcholine receptors,  $\alpha 4\beta 4$  and  $\alpha 7$ , show differential agonist binding modes. *The Journal of Biological Chemistry*. **2011**; 286: 14618-14627. © The American Society for Biochemistry and Molecular Biology.*

#### 4.1 ABSTRACT

Nicotinic acetylcholine receptors (nAChR) are pentameric, neurotransmitter-gated ion channels responsible for rapid excitatory neurotransmission in the central and peripheral nervous systems, resulting in skeletal muscle tone and various cognitive effects in the brain. These complex proteins are activated by the endogenous neurotransmitter acetylcholine (ACh) as well as by nicotine and structurally related agonists. Activation and modulation of nAChRs have been implicated in the pathology of multiple neurological disorders, and as such, these proteins are established therapeutic targets. Our lab has reported that the muscle-type,  $\alpha 4\beta 2$ , and  $\alpha 7$  receptors bind agonist molecules via a cation- $\pi$  interaction.<sup>1-3</sup> This chapter describes our efforts to elucidate the agonist binding mechanism of the  $\alpha 4\beta 4$  receptor. Unnatural amino acid mutagenesis and chimeric  $\beta$  subunits were used to probe the respective contributions of the  $\alpha 4\beta 4$  principal and complementary binding components to agonist binding and receptor pharmacology. Here, we report that the  $\alpha 4\beta 4$  receptor utilizes a strong cation- $\pi$  interaction to a conserved tryptophan (TrpB) of the receptor for both ACh and nicotine, and nicotine participates in a strong hydrogen bond with a backbone carbonyl contributed by TrpB.

## 4.2 INTRODUCTION

Nicotinic acetylcholine receptors (nAChRs) belong to the Cys-loop superfamily of neurotransmitter-gated ion channels, which includes  $\gamma$ -aminobutyric acid (GABA<sub>A</sub> and GABA<sub>C</sub>), glycine (Gly), and serotonin type 3 (5-HT<sub>3</sub>) receptors. These transmembrane proteins are critical to proper rapid synaptic transmission in the central and peripheral nervous systems.<sup>4</sup> In fact, several nAChRs have been implicated in pathophysiology and/or therapy of multiple neurological and psychiatric disorders including addiction, schizophrenia, Parkinson's disease, Alzheimer's disease, pain, ADHD, epilepsy, depression, and congenital myasthenic syndromes.<sup>5,6</sup>

The nAChR is the longest-known, most-studied neuroreceptor. nAChRs are pentameric, integral membrane proteins whose overall structure has been roughly determined by cryo-electron microscopy images of the *Torpedo californica* nAChR (**Figure 4.1**).<sup>7</sup> Each subunit contains a large, principally  $\beta$ -sheet extracellular N-terminal domain, four transmembrane  $\alpha$ -helices (M1-M4), and a small extracellular C-terminal domain. Five homologous subunits are arranged pseudosymmetrically around a central ion conducting pore formed by the M2 helices of each subunit.<sup>8</sup> To date, 16 mammalian genes have been identified that encode nAChR subunits, termed  $\alpha$ 1- $\alpha$ 7,  $\alpha$ 9,  $\alpha$ 10,  $\beta$ 1- $\beta$ 4,  $\delta$ ,  $\gamma$ , and  $\epsilon$ .

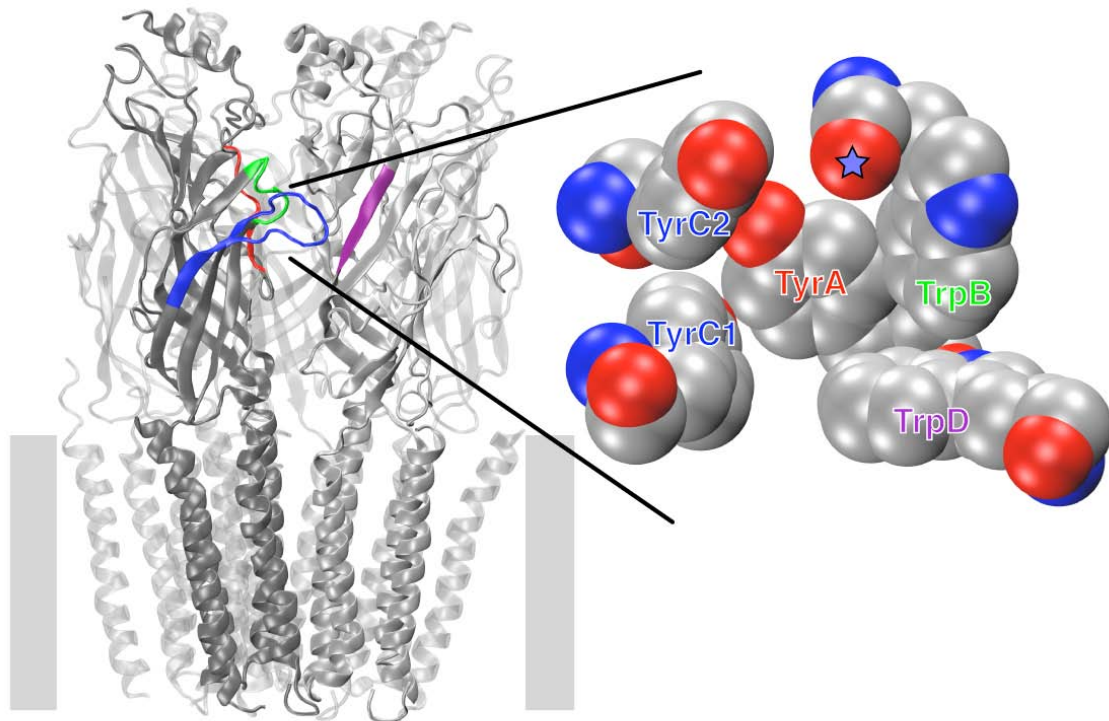


**Figure 4.1.** nAChR structure. *Left panel*, global layout of the nAChR based on cryo-electron microscopy of the *Torpedo* receptor (pdb: 2BG9).<sup>7</sup> The position of the membrane is denoted by gray bars. A large intracellular domain that is only partly observed in the structure is omitted. *Right panel*, enlargement of agonist binding site from AChBP (pdb: 1I9B).<sup>9</sup> Aromatic residues forming the ligand binding site are indicated. TyrA, TrpB, TyrC1, and TyrC2 are contributed by the  $\alpha$  subunit, and TrpD is contributed by the non- $\alpha$  subunit. Coloring of the residue labels matches that of the corresponding loops in the full structure. Backbone carbonyl contributed by TrpB is denoted by a star.

The “muscle-type” nAChR is postsynaptically located at the neuromuscular junction and has a uniquely precise stoichiometry of  $(\alpha 1)_2\beta 1\gamma\delta$  (fetal form; the adult form is  $(\alpha 1)_2\beta 1\epsilon\delta$ ). Neuronal nAChRs, however, are formed from various combinations of  $\alpha 2$ - $\alpha 10$  and  $\beta 2$ - $\beta 4$  subunits and current estimates indicate that as many as 25 active subtypes occur in humans.<sup>10, 11</sup> These receptors are mostly located post- and presynaptically in autonomic ganglia and cholinergic neurons of the CNS, but can also occur in non-neuronal cells.<sup>5, 10</sup> Given this large collection of closely related receptors, it

seems certain that therapeutics directed toward specific neurological disorders will require selectivity in terms of which nAChR subtype(s) is targeted.

Early work established a nicotinic pharmacophore comprised of a cationic N and a hydrogen bond accepting group separated by an appropriate distance.<sup>12, 13</sup> This report focuses on critical drug-receptor interactions occurring at the agonist binding site. The cationic moiety of ACh interacts with a cluster of aromatic amino acids first identified by photoaffinity labeling and mutagenesis experiments of the full receptor.<sup>4, 9</sup> Crystal structures of the acetylcholine binding proteins (AChBP) provided a structural template for the N-terminal, extracellular, ligand binding domain (LBD) of the nAChR, as it shares 20%-25% sequence identity with the extracellular domain of the much larger ion channel protein.<sup>9, 14</sup> Five aromatic residues (labeled according to their respective loop) form the agonist binding site, and these five aromatics are completely conserved across the nAChR family (**Figure 4.1**). The principal binding site contributes loop A (TyrA), loop B (TrpB), and loop C (TyrC1 and TyrC2), and the complementary binding site contributes loop D (TrpD), loop E, and loop F. In recent work, it was confirmed that the hydrogen bond acceptor of the agonist interacts with residues from the complementary subunits ( $\beta$  in neuronal nAChRs;  $\gamma$ ,  $\delta$ ,  $\varepsilon$  in the muscle-type nAChR).<sup>15</sup>

In the Dougherty group, we have used the nonsense suppression methodology to probe the molecular determinants for agonist binding in several nAChR subtypes, such as the muscle-type and neuronal  $\alpha 4\beta 2$  and  $\alpha 7$  receptors.<sup>1-3, 16, 17</sup> From these studies, the cation- $\pi$  interaction proved a common component of agonist affinity in each of the aforementioned receptors. Preliminary studies of the neuronal  $\alpha 4\beta 4$  nAChR, however, proved inconclusive.<sup>18</sup> Interestingly, the  $\alpha 4$  and  $\beta 4$  subunits colocalize in brain regions

implicated in behavioral responses to nicotine, and  $\beta 4^{-/-}$  knockout mice are more resistant to nicotine-induced seizures when compared to wild type mice.<sup>5, 19</sup> Given the significance of the  $\alpha 4\beta 4$  subtype in nicotine addiction and its similar structure to  $\alpha 4\beta 2$ , we were interested in elucidating the agonist binding mode of the  $\alpha 4\beta 4$  receptor.

The primary goal of the present work is described in two parts: (1) to use unnatural amino acid mutagenesis to probe the  $\alpha 4\beta 4$  principal binding site and determine the contribution of each residue (*e.g.*, TyrA, TrpB, TyrC1, and TyrC2) to agonist binding, and (2) to employ chimeric  $\beta$  subunits to identify which region(s) of the complementary binding site contributes to the divergent pharmacologies observed for the  $\alpha 4\beta 2$  and  $\alpha 4\beta 4$  receptors.

## 4.3 RESULTS

### 4.3.1 Part 1: Using Unnatural Amino Acid Mutagenesis to Probe the Principal Binding Site of the Neuronal $\alpha 4\beta 4$ Receptor

#### *Challenges in Studying Neuronal nAChRs with Unnatural Amino Acids*

The nonsense suppression methodology for incorporating unnatural amino acids into receptors and ion channels expressed in *Xenopus* oocytes has proven to be broadly applicable, including studies of serotonin (5-HT<sub>3</sub>) receptors, GABA receptors, glycine receptors, K<sup>+</sup> and Na<sup>+</sup> channels, and GPCRs.<sup>16, 20-24</sup> Studies of the muscle-type nAChR have long been straightforward, but attempts to apply the methodology to neuronal nAChRs were initially frustrated by several factors. These issues include poor expression in *Xenopus* oocytes as well as expression of variable stoichiometries. Here, we report the strategies used to overcome these obstacles in the  $\alpha 4\beta 4$  receptor.

Human  $\alpha 4$  and  $\beta 4$  subunit genes were in plasmid Bluescript (pBluescript). Injection of mRNA transcribed from pBluescript into oocytes produced moderate expression of wild type protein and low expression for nonsense suppression experiments. As such, both  $\alpha 4$  and  $\beta 4$  subunit genes were subcloned into pGEMhe facilitating *in vitro* transcription of mRNA for expression in *Xenopus* oocytes. Using mRNA transcribed from the pGEMhe vector, we successfully incorporated several unnatural amino acids into the  $\alpha 4\beta 4$  nAChR.

An additional issue concerning the expression of neuronal nAChRs in *Xenopus* oocytes is the tendency of these receptors to exist in variable stoichiometries. This can be problematic, since interpretation of subtle structure-function studies requires a homogeneous collection of receptors. Several studies of other receptor subtypes have shown that biasing the ratios of subunit mRNAs injected into the oocyte can influence subunit stoichiometry,<sup>2, 25</sup> and we have found similar results in our previous studies of unnatural amino acids in the  $\alpha 4\beta 2$  receptor.<sup>2</sup> For the  $\alpha 4\beta 2$  nAChR, the  $(\alpha 4)_2(\beta 2)_3$  form is the higher sensitivity form for nicotine, and chronic exposure to nicotine leads to upregulation of this form at the expense of  $(\alpha 4)_3(\beta 2)_2$  in a variety of cell types.<sup>25, 26</sup>

In initial studies of the  $\alpha 4\beta 4$  receptor, we observed variable dose-response curves and anomalously low Hill coefficients, indicating a mixed population of receptors. By biasing the subunit mRNA ratios, we observed two dominant  $\alpha 4\beta 4$  receptor populations, which we have assigned as  $(\alpha 4)_2(\beta 4)_3$  and  $(\alpha 4)_3(\beta 4)_2$ . In order to facilitate comparisons and to emphasize the critical role of the  $\beta$  subunit in defining drug selectivity at nAChRs, our studies of the  $\alpha 4\beta 4$  nAChR have focused on the  $(\alpha 4)_2(\beta 4)_3$  form. We found that injection of an mRNA ratio  $\alpha 4:\beta 4$  of 1:1 or lower produces a pure population of

$(\alpha 4)_2(\beta 4)_3$ , while a ratio greater than 30:1 is necessary to produce pure populations of  $(\alpha 4)_3(\beta 4)_2$  (**Table 4.1**).

**Table 4.1.** Stoichiometries of  $\alpha 4\beta 4$  nAChRs expressed in *Xenopus* oocytes injected with different ratios of human  $\alpha 4:\beta 4$  subunit mRNA.  $EC_{50}$  ( $\mu M$ ) and  $n_H$  values are  $\pm SEM$ .

<b>Ratio</b>	<b>ACh</b>	<b><math>n_H</math></b>	<b>Stoichiometry</b>
<b>100:1</b>	$58 \pm 3$	$1.9 \pm 0.2$	A3B2
<b>30:1</b>	$51 \pm 3$	$1.9 \pm 0.2$	Mixture
<b>10:1</b>	$41 \pm 2$	$1.4 \pm 0.1$	Mixture
<b>3:1</b>	$26 \pm 1$	$1.1 \pm 0.1$	Mixture
<b>1:1</b>	$11 \pm 1$	$1.3 \pm 0.1$	A2B3
<b>1:3</b>	$13 \pm 1$	$1.3 \pm 0.1$	A2B3
<b>Ratio</b>	<b>Nicotine</b>	<b><math>n_H</math></b>	<b>Stoichiometry</b>
<b>100:1</b>	$12 \pm 2$	$1.7 \pm 0.3$	A3B2
<b>1:3</b>	$2.4 \pm 0.1$	$1.3 \pm 0.1$	A2B3

With the above strategies, unnatural amino acid mutagenesis studies of the  $\alpha 4\beta 4$  receptor proceeded smoothly (**Figure 4.2**). In the present work, we report  $EC_{50}$  measurements, the effective concentration of agonist required to induce half-maximal response.  $EC_{50}$  is a functional measure that can be altered by changes in agonist affinity and/or receptor gating. All of our previous studies of the nAChR agonist binding site have employed this metric, and so using  $EC_{50}$  values allows direct comparisons between different subtypes. In addition, an earlier study of the  $\alpha 4\beta 2$  receptor employed single-channel analysis to establish that shifts in  $EC_{50}$  caused by subtle mutations at TrpB, a major focus of the present work, result from changes in agonist affinity, not receptor gating.<sup>2</sup>

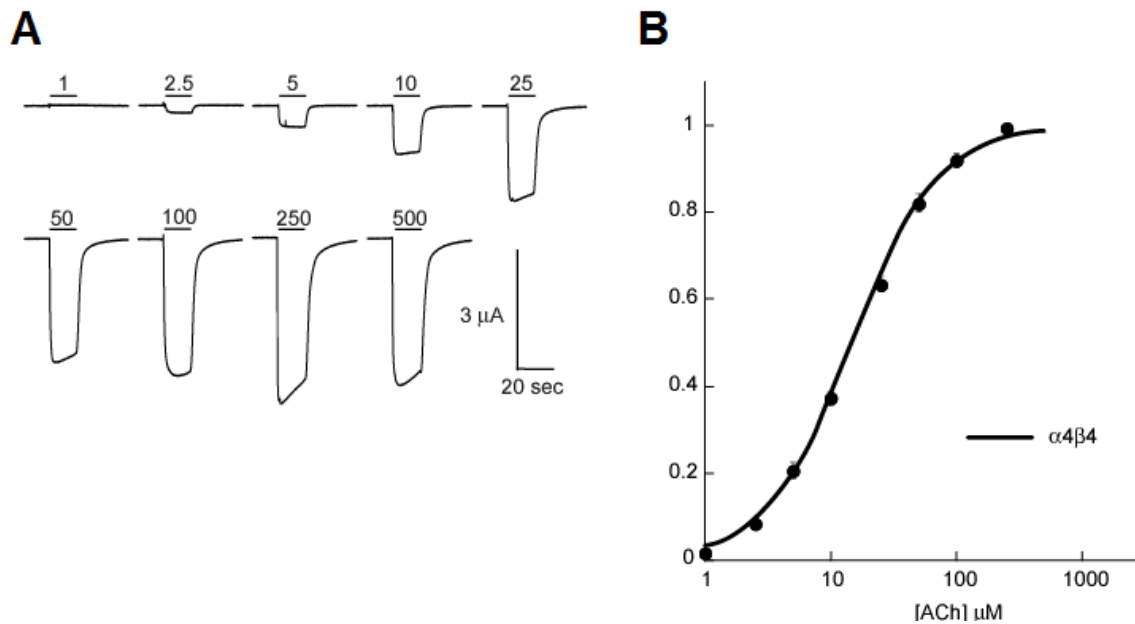


**Figure 4.2.** Wild type recovery experiments for the  $\alpha 4\beta 4$  nAChR. A. Representative voltage-clamp current traces from oocytes with Trp incorporated by nonsense suppression at position TrpB. Bars indicate application of ACh at concentrations ( $\mu\text{M}$ ) noted. B. Dose-response curve and fit of data in A to the Hill equation. Error bars indicate SEM.;  $n = 10\text{-}13$ .

#### *Ligand Binding Mechanism of the $\alpha 4\beta 4$ Receptor*

Our lab has previously established that the muscle-type and  $\alpha 4\beta 2$  nAChRs interact with agonists (**Figure 4.3A**) through cation- $\pi$  interactions at TrpB.<sup>2, 3</sup> We therefore focused on TrpB in the  $\alpha 4\beta 4$  receptor using strategies that are now well established for identifying a cation- $\pi$  interaction. In particular, we systematically fluorinate a side chain (**Figure 4.3B**) and determine whether the progressive diminution of the cation- $\pi$  binding ability of the residue induced by fluorination is manifested in receptor function. The fluorination approach can be augmented with other substitutions, such as the highly deactivating cyano (CN) substituent, and is compared to the much less deactivating but sterically similar bromo (Br) substituent. With ACh as agonist, both the CN-Trp/Br-Trp effect (9-fold ratio of  $\text{EC}_{50}$ ; **Table 4.2**) and the fluorination effect (**Figure**

**4.4A)** establish that a cation- $\pi$  interaction is present at TrpB. We were unable to achieve adequate incorporation of F<sub>3</sub>-Trp or F<sub>4</sub>-Trp, so we incorporated 7-aza-Trp, which is structurally very similar to Trp but shows a diminished cation- $\pi$  binding ability. When all the data are combined (Trp, F<sub>1</sub>-Trp, F<sub>2</sub>-Trp, 7-aza-Trp, Br-Trp, and CN-Trp) into one plot, we observe a linear correlation with *ab initio* calculated cation- $\pi$  binding energies. The slope of this cation- $\pi$  binding plot resembles that reported for other nAChRs. A much more thorough study was possible with nicotine as the agonist, producing compelling evidence for a cation- $\pi$  interaction to TrpB (**Figure 4.4B**). Considering the effects of nicotine at TrpB, the cation- $\pi$  slope resembles that of the  $\alpha$ 4 $\beta$ 2 receptor rather than the muscle-type receptor, which shows no consistent fluorination effect with nicotine as the agonist. Hence, in the  $\alpha$ 4 $\beta$ 4 receptor, similar to the  $\alpha$ 4 $\beta$ 2 receptor,<sup>2</sup> nicotine mimics ACh at TrpB with regard to the cation- $\pi$  interaction.

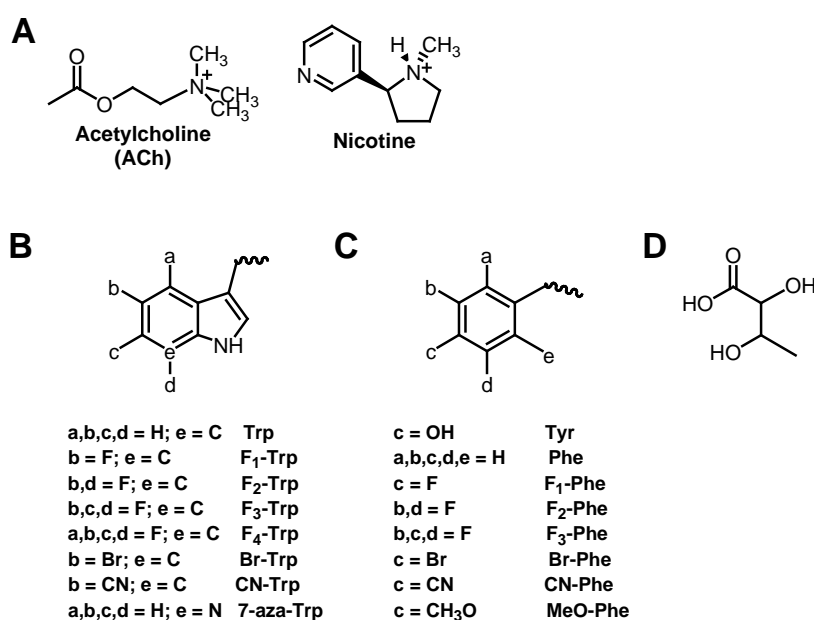


**Figure 4.3.** Key structures employed in this study. A. Structures of ACh and nicotine. B. Tryptophan derivatives; F<sub>1</sub>-Trp, 5-fluoro-tryptophan; F<sub>2</sub>-Trp, 5,7-difluoro-tryptophan; F<sub>3</sub>-Trp, 5,6,7-trifluoro-tryptophan; F<sub>4</sub>-Trp, 4,5,6,7-tetrafluoro-tryptophan; Br-Trp, 5-bromo-tryptophan; CN-Trp, 5-cyano-tryptophan; 7-aza-Trp, 7-aza-tryptophan. C. Phenylalanine

derivatives; F<sub>1</sub>-Phe, 4-fluoro-phenylalanine; F<sub>2</sub>-Phe, 3,5-difluoro-phenylalanine; F<sub>3</sub>-Phe, 3,4,5-trifluoro-phenylalanine; Br-Phe, 4-bromo-phenylalanine; CN-Phe, 4-cyano-phenylalanine; MeO-Phe, 4-methoxy-phenylalanine. If not indicated, a, b, c, or d group is H. D. Tah, threonine- $\alpha$ -hydroxy.

**Table 4.2.** Data for mutant  $\alpha 4\beta 4$  (A2B3) nAChRs.  $EC_{50}$  ( $\mu M$ ) and  $n_H$  values are  $\pm SEM$ . NR = No response.

<b>Mutation</b>	<b>ACh</b>	<b><math>n_H</math></b>	<b>Nicotine</b>	<b><math>n_H</math></b>
<b>(<math>\alpha 4</math>)<sub>3</sub>(<math>\beta 4</math>)<sub>2</sub></b>	58 $\pm$ 3	1.9 $\pm$ 0.2	12 $\pm$ 2	1.7 $\pm$ 0.3
<b>(<math>\alpha 4</math>)<sub>2</sub>(<math>\beta 4</math>)<sub>3</sub></b>	13 $\pm$ 1	1.3 $\pm$ 0.1	2.4 $\pm$ 0.1	1.3 $\pm$ 0.1
<b>TyrA</b>				
<b>Tyr</b>	17 $\pm$ 1	1.2 $\pm$ 0.1	3.1 $\pm$ 0.2	1.3 $\pm$ 0.1
<b>Phe</b>	260 $\pm$ 11	1.3 $\pm$ 0.1	11 $\pm$ 0.4	1.6 $\pm$ 0.1
<b>F<sub>1</sub>-Phe</b>	254 $\pm$ 21	1.3 $\pm$ 0.1	6.6 $\pm$ 0.6	1.5 $\pm$ 0.2
<b>F<sub>2</sub>-Phe</b>	159 $\pm$ 16	1.3 $\pm$ 0.1	7.1 $\pm$ 0.4	1.4 $\pm$ 0.1
<b>F<sub>3</sub>-Phe</b>	158 $\pm$ 14	1.4 $\pm$ 0.1	7.7 $\pm$ 0.5	1.4 $\pm$ 0.1
<b>Br-Phe</b>	49 $\pm$ 1	1.6 $\pm$ 0.1	3.5 $\pm$ 0.2	1.5 $\pm$ 0.1
<b>CN-Phe</b>	855 $\pm$ 63	1.4 $\pm$ 0.1	80 $\pm$ 6	1.4 $\pm$ 0.1
<b>MeO-Phe</b>	50 $\pm$ 2	1.4 $\pm$ 0.1	4.2 $\pm$ 0.2	1.4 $\pm$ 0.1
<b>TrpB</b>				
<b>Trp</b>	15 $\pm$ 1	1.3 $\pm$ 0.1	2.0 $\pm$ 0.1	1.2 $\pm$ 0.1
<b>F<sub>1</sub>-Trp</b>	41 $\pm$ 2	1.5 $\pm$ 0.1	5.6 $\pm$ 0.5	1.4 $\pm$ 0.1
<b>F<sub>2</sub>-Trp</b>	51 $\pm$ 2	1.6 $\pm$ 0.1	8.1 $\pm$ 0.9	1.5 $\pm$ 0.2
<b>F<sub>3</sub>-Trp</b>	NR	NR	73 $\pm$ 6	1.2 $\pm$ 0.1
<b>F<sub>4</sub>-Trp</b>	NR	NR	190 $\pm$ 116	0.8 $\pm$ 0.2
<b>Br-Trp</b>	28 $\pm$ 1	1.5 $\pm$ 0.1	7.1 $\pm$ 0.5	1.5 $\pm$ 0.1
<b>CN-Trp</b>	254 $\pm$ 27	1.2 $\pm$ 0.1	46 $\pm$ 3	1.6 $\pm$ 0.1
<b>7-aza-Trp</b>	162 $\pm$ 17	1.6 $\pm$ 0.2	28 $\pm$ 2	2.0 $\pm$ 0.2
<b>TyrC1</b>				
<b>Tyr</b>	11 $\pm$ 1	1.2 $\pm$ 0.1	1.8 $\pm$ 0.1	1.3 $\pm$ 0.1
<b>Phe</b>	1100 $\pm$ 126	1.8 $\pm$ 0.3	60 $\pm$ 2	2.0 $\pm$ 0.1
<b>Br-Phe</b>	1400 $\pm$ 140	2.0 $\pm$ 0.3	65 $\pm$ 9	1.3 $\pm$ 0.2
<b>CN-Phe</b>	2700 $\pm$ 500	1.5 $\pm$ 0.2	156 $\pm$ 13	1.8 $\pm$ 0.2
<b>MeO-Phe</b>	550 $\pm$ 37	1.6 $\pm$ 0.1	75 $\pm$ 9	1.5 $\pm$ 0.2
<b>TyrC2</b>				
<b>Tyr</b>	11 $\pm$ 1	1.2 $\pm$ 0.1	2.2 $\pm$ 0.1	1.3 $\pm$ 0.1
<b>Phe</b>	26 $\pm$ 1	1.6 $\pm$ 0.1	2.0 $\pm$ 0.2	1.6 $\pm$ 0.2
<b>Br-Phe</b>	4.5 $\pm$ 0.3	1.4 $\pm$ 0.1	0.36 $\pm$ 0.01	1.7 $\pm$ 0.1
<b>CN-Phe</b>	11 $\pm$ 1	1.2 $\pm$ 0.1	2.5 $\pm$ 0.1	1.4 $\pm$ 0.1
<b>MeO-Phe</b>	13 $\pm$ 1	1.3 $\pm$ 0.1	1.3 $\pm$ 0.1	1.5 $\pm$ 0.2
<b>Thr(B+1)</b>				
<b>Thr</b>	15 $\pm$ 1	1.3 $\pm$ 0.1	1.7 $\pm$ 0.1	1.3 $\pm$ 0.1
<b>Tah</b>	12 $\pm$ 1	1.3 $\pm$ 0.1	23 $\pm$ 1	1.6 $\pm$ 0.1

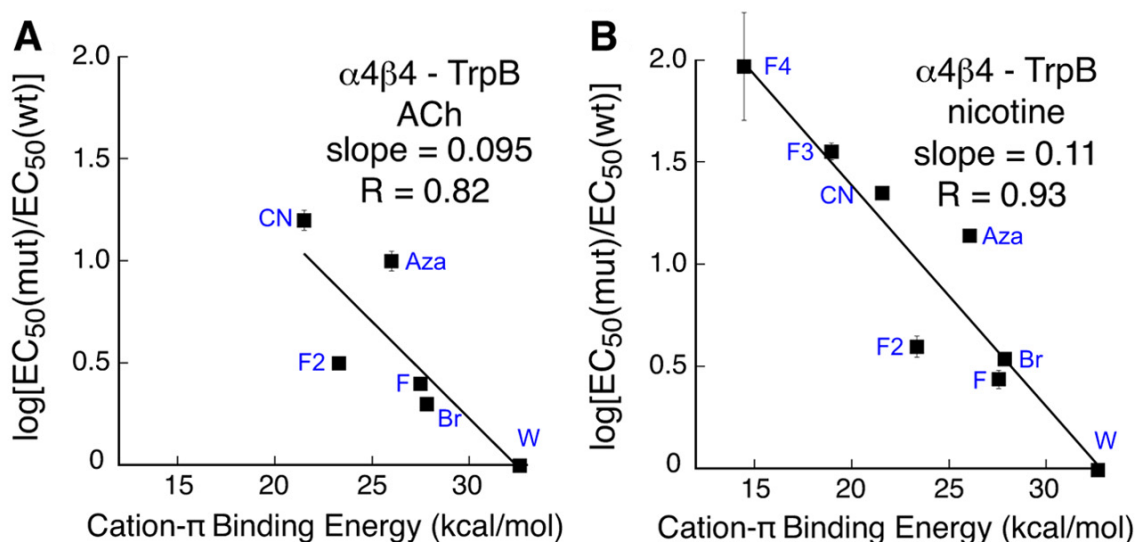


**Figure 4.4.** Cation- $\pi$  binding plots for  $\alpha 4\beta 4$  nAChR at position TrpB with ACh (A) and nicotine (B).  $\text{Log}[EC_{50}(\text{mut})/EC_{50}(\text{wt})]$  is plotted *vs.* quantitative cation- $\pi$  binding energies.<sup>3</sup> Data are from Table 4.2. Where not visible, error bars are smaller than the data marker.

We performed extensive studies of the remaining components of the aromatic box contributed by the principal face of the ligand binding domain (TyrA, TyrC1, and TyrC2). Historically, nonsense suppression with tyrosine derivatives has proven more challenging than tryptophan derivatives when probing for a cation- $\pi$  interaction. Direct fluorination of tyrosine progressively lowers the  $\text{pK}_a$  of the side chain hydroxyl group, such that the  $\text{pK}_a$  for tetrafluorotyrosine is  $\sim 5.3$  (lowered from  $\sim 10$  for tyrosine). This decrease in  $\text{pK}_a$  can lead to ionization of the hydroxyl in unnatural tyrosine analogues. Thus observed shifts in  $EC_{50}$  could result from ionization of the hydroxyl group rather than changes in the cation- $\pi$  binding ability, complicating analysis. In other receptors, we have circumvented this potential problem by first incorporating phenylalanine, followed by successively fluorinated phenylalanine derivatives (**Figure 4.3C**), thereby avoiding the  $\text{pK}_a$  complication.<sup>27</sup>

In the  $\alpha 4\beta 4$  receptor, we found that for TyrA deletion of the hydroxyl group (to give Phe) severely impacts receptor function for both ACh and nicotine (**Table 4.2**). Incorporation of either MeO-Phe or Br-Phe perturbs receptor function minimally, while CN-Phe is strongly perturbing. This represents a distinction in the behavior of TyrA when comparing  $\alpha 4\beta 4$  to the  $\alpha 4\beta 2$  and muscle-type receptors. For proper receptor function in  $\alpha 4\beta 4$ , it appears that TyrA requires only steric bulk at this position. However, MeO-Phe is highly deleterious in the  $\alpha 4\beta 2$  and muscle-type receptors, suggesting a hydrogen bond donor is required. Successive fluorination of phenylalanine does not result in progressively reduced channel function; we conclude that neither ACh nor nicotine participates in a cation- $\pi$  interaction with TyrA.

The remaining two residues, TyrC1 and TyrC2, are both contributed by loop C, a very mobile component of the binding site.<sup>28</sup> We probed both of these residues for possible hydrogen bonding and cation- $\pi$  interactions, and we find that TyrC1 and TyrC2 display opposite effects. TyrC1 is highly sensitive to any mutation that obliterates hydrogen bond donating ability, as evidenced by a rightward shift in  $EC_{50}$  of over 50-fold for ACh and 30-fold for nicotine in response to the Phe, MeO-Phe, Br-Phe, and CN-Phe mutations (**Table 4.2**). Given the small CN-Phe/Br-Phe ratio, TyrC1 is not likely to interact with either ACh or nicotine through a cation- $\pi$  interaction. If this position served as a hydrogen bond acceptor, then incorporation of MeO-Phe would have rescued normal channel function. Rather, MeO-Phe incorporation resulted in a substantial loss of channel function; therefore, we conclude that TyrC1 is an important hydrogen bond donor.

In contrast, TyrC2 is quite receptive to mutations of the 4-position hydroxyl group, with many types of substituents accepted and no obvious structure-function relationship. The fact that CN-Phe gives essentially wild type behavior for both ACh and nicotine would appear to rule out a strong cation- $\pi$  interaction at this site. These results suggest that TyrC2 participates structurally in shaping the ligand-binding site rather than directly in ligand recognition. Again, the results for both TyrC1 and TyrC2 are similar to what is seen for muscle-type and  $\alpha 4\beta 2$ .

In  $\alpha 4\beta 4$ , we also investigated the hydrogen bonding capability of the backbone carbonyl of TrpB (**Figure 4.1**), because this site is known to behave differently in the muscle-type and  $\alpha 4\beta 2$  nAChRs.<sup>2, 17</sup> By replacing the amino acid at the *i+1* position with the analogous  $\alpha$ -hydroxy acid, one converts the carbonyl associated with residue *i* to an ester carbonyl rather than an amide (peptide) carbonyl (**Figure 4.5, Figure 4.3D**).<sup>17</sup> It is well established that ester carbonyls are poorer hydrogen bond acceptors than amide carbonyls, and so if a hydrogen bond to this carbonyl is essential, the backbone ester mutation should influence agonist potency. With nicotine as the agonist, the backbone ester mutation causes a 14-fold increase in EC<sub>50</sub> in  $\alpha 4\beta 4$  (**Table 4.2**). Importantly, the potency of ACh, which cannot make a conventional hydrogen bond to the carbonyl, is essentially unperturbed by the backbone ester mutation. This establishes that the mutation does not globally alter the binding/gating characteristics of the receptor, supporting the notion that we are modulating a hydrogen bonding interaction between the receptor and nicotine. As with TrpB, the behavior of  $\alpha 4\beta 4$  is more similar to that of  $\alpha 4\beta 2$  rather than muscle-type.

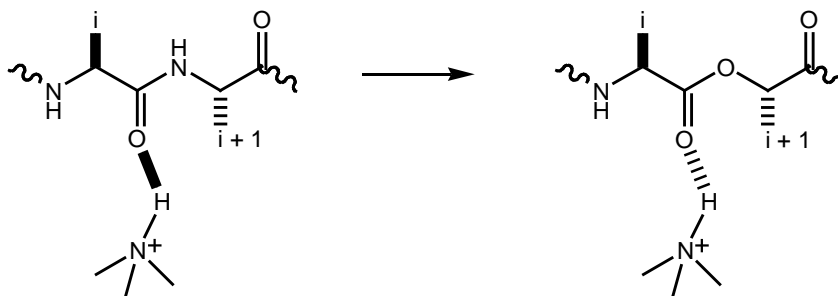


**Figure 4.5.** The backbone ester strategy for modulating a hydrogen bond;  $\alpha$ -hydroxy acid incorporation.

### 4.3.2 Part 2: Using Chimeric $\beta$ Subunits to Examine the Contribution of the Complementary Binding Site to Subtype-Specific Receptor Pharmacology

We have now established that  $\alpha 4\beta 2^2$  and  $\alpha 4\beta 4$  utilize the same drug-receptor interactions to bind agonists (*e.g.*, a cation- $\pi$  interaction and a hydrogen bond). However, several studies have suggested that the subtle pharmacological differences observed for these neuronal nAChRs are determined by the identities of both the  $\alpha$  and  $\beta$  subunits.<sup>29-31</sup> Given that both  $\alpha 4\beta 2$  and  $\alpha 4\beta 4$  receptors contain an identical principal binding site contributed by the  $\alpha 4$  subunit, the complementary subunit (*i.e.*,  $\beta 4$  vs.  $\beta 2$ ) is likely the discriminating factor amongst these two receptors. In fact, studies by Parker *et al.* confirmed that  $\beta 2$ -containing receptors consistently display higher affinities for agonists compared to  $\beta 4$ -containing receptors, and identified loop D as a major determinant for agonist affinity.<sup>31</sup> In part 2 of this chapter, we use chimeric  $\beta$  subunits to identify which loop(s) of the complementary binding site influences agonist binding and receptor pharmacology.

#### **General Strategy**

The complementary binding site was partitioned into discrete sections according to loops D-F, and several chimeric  $\beta$  subunits were designed, replacing portions of the  $\beta 2$

subunit with the corresponding region from the  $\beta 4$  subunit (**Figure 4.6**). Chimera D converted loop D of the  $\beta 2$  subunit to that of the  $\beta 4$  subunit via a single semiconserved threonine to lysine mutation. Similarly, chimeras E and F replaced either loop E or F to the analogous  $\beta 4$  region to examine their respective effects on agonist affinity. As shown in **Figure 4.6**, there is considerable residue variety among the sequences of loops E and F. In combination, these mutations may account for subtle changes in the ligand binding site and ultimately affect pharmacological properties of the receptor. The four remaining chimeras (DE, DF, EF, and DEF) replaced multiple loops of the  $\alpha 4\beta 2$  complementary binding site with the corresponding  $\beta 4$  loops. Chimera DEF completely converts the  $\alpha 4\beta 2$  agonist binding site to that of  $\alpha 4\beta 4$ .

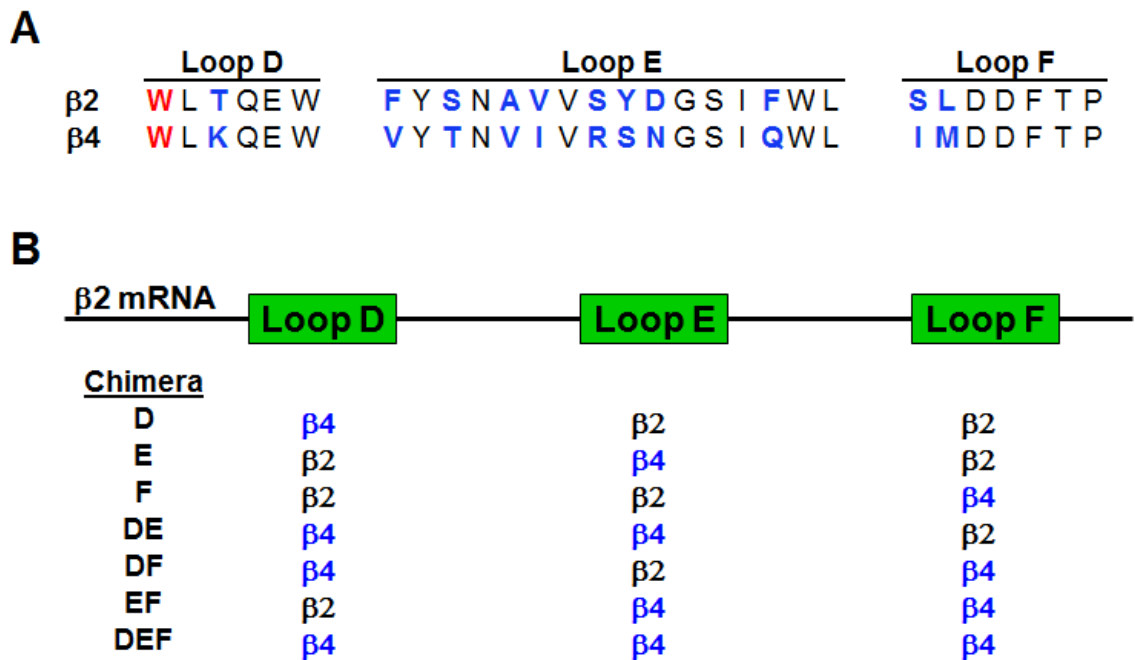


**Figure 4.6.** Design of chimeric  $\beta$  subunits. A. Complementary LBD loop sequences for rat  $\beta 2$  and  $\beta 4$  subunits. TrpD is highlighted in red. Differences in the sequences are highlighted in blue. B. Depiction of chimeras constructed from various combinations  $\beta 2$  and  $\beta 4$  regions.

All chimeric  $\beta$  subunits were coexpressed with the  $\alpha 4$  subunit. In accordance with previous studies of  $\alpha 4\beta 2$  and  $\alpha 4\beta 4$ ,<sup>1, 2</sup> a  $\alpha 4$ :chimeric  $\beta$  mRNA ratio of 1:3 ratio was coinjected into oocytes to ensure a homogeneous population of  $(\alpha 4)_2(\beta 2/\beta 4)_3$  receptors. In both  $\alpha 4\beta 2$  and  $\alpha 4\beta 4$ , TrpB is the key residue that interacts with both ACh and nicotine via a cation- $\pi$  interaction, a key component of agonist binding.<sup>2</sup> We therefore incorporated F<sub>3</sub>-Trp at TrpB in each chimeric receptor and evaluated the impact on the cation- $\pi$  interaction. For chimeras that experienced a functional change in response F<sub>3</sub>-Trp incorporation when compared to  $\alpha 4\beta 2$ , additional tryptophan derivatives were incorporated at TrpB (**Figure 4.3B**).

#### ***Functional Scan of Chimeric $\alpha 4\beta 2/\beta 4$ Receptors***

EC<sub>50</sub> was used to evaluate receptor function as discussed in Part 1. Although EC<sub>50</sub> is composed of both binding and gating parameters, we anticipate that shifts in EC<sub>50</sub> caused by subtle mutations at TrpB result from changes in agonist binding, not receptor gating, based on previous single-channel analysis of  $\alpha 4\beta 2$ .<sup>2</sup> Using either ACh or nicotine as the agonist, a dose-response relationship was determined for each chimera. EC<sub>50</sub> values of chimeric receptors were compared to  $\alpha 4\beta 2$  values (**Table 4.3**). Each chimera was functional and EC<sub>50</sub> values were slightly shifted from  $\alpha 4\beta 2$ , with chimera DE experiencing the greatest perturbation.

**Table 4.3.** EC<sub>50</sub> values ( $\mu\text{M}$ ) and Hill coefficients for  $\alpha 4\beta 2/\beta 4$  chimeras. All values are  $\pm$ S.E. †Previously reported in Xiu 2009.<sup>2</sup> All other values in this table were determined in the present work.

		ACh	n <sub>H</sub>	Nicotine	n <sub>H</sub>	Norm. I (+70mV)
$(\alpha 4)_3(\beta 2)_2^\dagger$		0.023 $\pm$ 0.001	1.3 $\pm$ 0.1	0.01 $\pm$ 0.001	1.7 $\pm$ 0.2	0.297 $\pm$ 0.041
$(\alpha 4)_2(\beta 2)_3^\dagger$		0.42 $\pm$ 0.01	1.2 $\pm$ 0.1	0.08 $\pm$ 0.01	1.2 $\pm$ 0.1	0.041 $\pm$ 0.005
Chimera	Mutation					
<b>D</b>	Wild Type ( <b>D</b> )	0.31 $\pm$ 0.01	1.4 $\pm$ 0.1	0.09 $\pm$ 0.01	1.5 $\pm$ 0.1	0.022 $\pm$ 0.005
	Trp	0.39 $\pm$ 0.01	1.4 $\pm$ 0.1	0.09 $\pm$ 0.01	1.4 $\pm$ 0.1	-0.006 $\pm$ 0.017
	F <sub>3</sub> -Trp	30 $\pm$ 1	1.6 $\pm$ 0.1	2.1 $\pm$ 0.1	1.2 $\pm$ 0.1	0.031 $\pm$ 0.010
<b>E</b>	Wild type ( <b>E</b> )	0.69 $\pm$ 0.02	1.4 $\pm$ 0.1	0.23 $\pm$ 0.02	1.9 $\pm$ 0.2	0.019 $\pm$ 0.004
	Trp	0.83 $\pm$ 0.03	1.3 $\pm$ 0.1	0.23 $\pm$ 0.02	1.6 $\pm$ 0.2	0.006 $\pm$ 0.011
	F <sub>3</sub> -Trp	46 $\pm$ 3	1.3 $\pm$ 0.1	10 $\pm$ 1	1.2 $\pm$ 0.2	0.015 $\pm$ 0.006
<b>F</b>	Wild type ( <b>F</b> )	0.11 $\pm$ 0.01	1.1 $\pm$ 0.1	0.09 $\pm$ 0.01	1.3 $\pm$ 0.1	0.018 $\pm$ 0.011
	Trp	0.10 $\pm$ 0.01	1.2 $\pm$ 0.1	0.06 $\pm$ 0.01	1.3 $\pm$ 0.1	0.040 $\pm$ 0.003
	F <sub>3</sub> -Trp	6.5 $\pm$ 0.3	1.1 $\pm$ 0.1	0.54 $\pm$ 0.03	1.5 $\pm$ 0.1	0.047 $\pm$ 0.008
<b>DE</b>	Wild type ( <b>DE</b> )	1.8 $\pm$ 0.1	1.4 $\pm$ 0.1	0.68 $\pm$ 0.03	1.6 $\pm$ 0.1	0.018 $\pm$ 0.005
	Trp	2.3 $\pm$ 0.1	1.3 $\pm$ 0.1	0.49 $\pm$ 0.03	1.7 $\pm$ 0.1	0.018 $\pm$ 0.004
	F <sub>3</sub> -Trp	130 $\pm$ 10	1.1 $\pm$ 0.1	20 $\pm$ 3	1.9 $\pm$ 0.4	0.018 $\pm$ 0.012
<b>DF</b>	Wild type ( <b>DF</b> )	0.21 $\pm$ 0.01	1.2 $\pm$ 0.1	0.07 $\pm$ 0.01	1.1 $\pm$ 0.1	0.021 $\pm$ 0.004
	Trp	0.16 $\pm$ 0.01	1.2 $\pm$ 0.1	0.04 $\pm$ 0.01	1.5 $\pm$ 0.1	0.039 $\pm$ 0.006
	F <sub>3</sub> -Trp	13 $\pm$ 1	1.4 $\pm$ 0.1	1.1 $\pm$ 0.1	1.4 $\pm$ 0.1	0.043 $\pm$ 0.003
<b>EF</b>	Wild type ( <b>EF</b> )	0.22 $\pm$ 0.01	1.4 $\pm$ 0.1	0.24 $\pm$ 0.01	1.8 $\pm$ 0.1	0.041 $\pm$ 0.006
	Trp	0.23 $\pm$ 0.01	1.1 $\pm$ 0.1	0.30 $\pm$ 0.01	1.8 $\pm$ 0.1	0.037 $\pm$ 0.006
	F <sub>3</sub> -Trp	46 $\pm$ 2	1.4 $\pm$ 0.1	15 $\pm$ 1	1.9 $\pm$ 0.2	0.071 $\pm$ 0.009
<b>DEF</b>	Wild type ( <b>DEF</b> )	0.55 $\pm$ 0.03	1.4 $\pm$ 0.1	0.39 $\pm$ 0.02	1.9 $\pm$ 0.1	0.005 $\pm$ 0.009
	Trp	0.5 $\pm$ 0.02	1.1 $\pm$ 0.1	0.42 $\pm$ 0.02	1.5 $\pm$ 0.1	0.035 $\pm$ 0.004
	F <sub>3</sub> -Trp	73 $\pm$ 3	1.5 $\pm$ 0.1	20 $\pm$ 1	1.8 $\pm$ 0.2	0.019 $\pm$ 0.003

For each chimeric receptor, F<sub>3</sub>-Trp was incorporated at TrpB to evaluate the impact of the altered complementary binding site on the native cation- $\pi$  interaction (a key component of the agonist binding mode) (**Table 4.3**). The F<sub>3</sub>-Trp/Trp fold shifts reported for  $\alpha 4\beta 2$  and  $\alpha 4\beta 4$  were compared to the fold shift for each chimera (**Figure 4.7**). A fold shift for ACh at  $\alpha 4\beta 4$  was unavailable due to inadequate incorporation of F<sub>3</sub>-Trp at TrpB. With ACh as agonist, all chimeras exhibited a F<sub>3</sub>-Trp/Trp fold shift greater than that observed for  $\alpha 4\beta 2$ . A similar trend was observed for nicotine, with one exception – chimera F. Here, the F<sub>3</sub>-Trp/Trp fold shift for chimera F was less than values observed for both  $\alpha 4\beta 2$  and  $\alpha 4\beta 4$ . This result was interesting; suggesting that chimera F disrupted

the cation- $\pi$  interaction as evidenced by a smaller perturbation in response to incorporation of F<sub>3</sub>-Trp (**Figure 4.7**). Although the effect was not large, chimera F was the obvious target for additional suppression experiments.

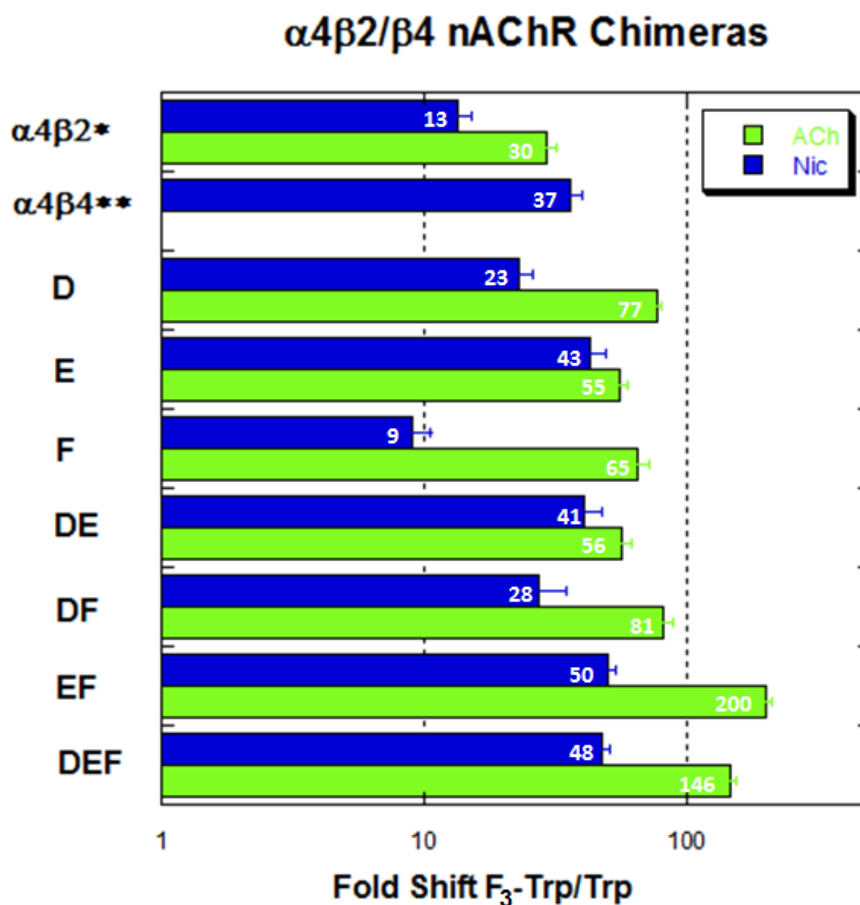


**Figure 4.7.** Bar graph comparing F<sub>3</sub>-Trp/Trp fold shifts for chimeric receptors. Fold shifts for ACh (green) and nicotine (blue) are indicated in white lettering. \*Previously reported in Xiu 2009.<sup>2</sup> \*\*Previously reported in Puskar 2011.<sup>1</sup> All other values in this table were determined in the present work.

#### *Using the Fluorination Approach to Explore the Effect of Loop F on Agonist Binding*

Given that ACh and nicotine responded differently to incorporation of F<sub>3</sub>-Trp at TrpB in chimera F, we used the fluorination approach to further examine the effect of chimera F on the cation- $\pi$  interaction at TrpB (as described in Part 1) (**Figure 4.3B**). The  $\log(\text{EC}_{50}(\text{mutant})/\text{EC}_{50}(\text{wild type}))$  was plotted against *ab initio* calculated cation- $\pi$

binding energies (Table 4.4).<sup>3</sup> Typically, we interpret the slope of a cation- $\pi$  binding plot to indicate the relative strength of a cation- $\pi$  interaction, and as such, we compared the slope obtained for chimera F to values observed for  $\alpha 4\beta 2$  and  $\alpha 4\beta 4$ .

**Table 4.4.** EC<sub>50</sub> values ( $\mu\text{M}$ ) and Hill coefficients for chimera F. All values are  $\pm$ S.E. F<sub>1</sub>-Trp, 5-fluoro-tryptophan; F<sub>2</sub>-Trp, 5,7-difluoro-tryptophan; F<sub>3</sub>-Trp, 5,6,7-trifluoro-tryptophan; F<sub>4</sub>-Trp, 4,5,6,7-tetrafluoro-tryptophan; Br-Trp, 5-bromo-tryptophan; CN-Trp, 5-cyano-tryptophan.

Mutation	ACh	n <sub>H</sub>	Nic	n <sub>H</sub>	Norm I (+70mV)
Trp	0.10 $\pm$ 0.01	1.2 $\pm$ 0.1	0.06 $\pm$ 0.01	1.3 $\pm$ 0.1	0.040 $\pm$ 0.003
F <sub>1</sub> -Trp	0.51 $\pm$ 0.02	1.3 $\pm$ 0.1	0.27 $\pm$ 0.01	1.4 $\pm$ 0.1	0.031 $\pm$ 0.011
F <sub>2</sub> -Trp	1.2 $\pm$ 0.1	1.1 $\pm$ 0.1	0.27 $\pm$ 0.01	1.3 $\pm$ 0.1	0.051 $\pm$ 0.009
F <sub>3</sub> -Trp	6.5 $\pm$ 0.3	1.1 $\pm$ 0.1	0.54 $\pm$ 0.03	1.5 $\pm$ 0.1	0.047 $\pm$ 0.008
F <sub>4</sub> -Trp	15 $\pm$ 1	1.1 $\pm$ 0.1	3.6 $\pm$ 0.3	1.0 $\pm$ 0.1	0.025 $\pm$ 0.007
Br-Trp	0.35 $\pm$ 0.02	1.4 $\pm$ 0.1	0.20 $\pm$ 0.01	1.6 $\pm$ 0.1	0.035 $\pm$ 0.005
CN-Trp	4.7 $\pm$ 0.2	1.3 $\pm$ 0.1	1.9 $\pm$ 0.2	1.4 $\pm$ 0.2	0.032 $\pm$ 0.005

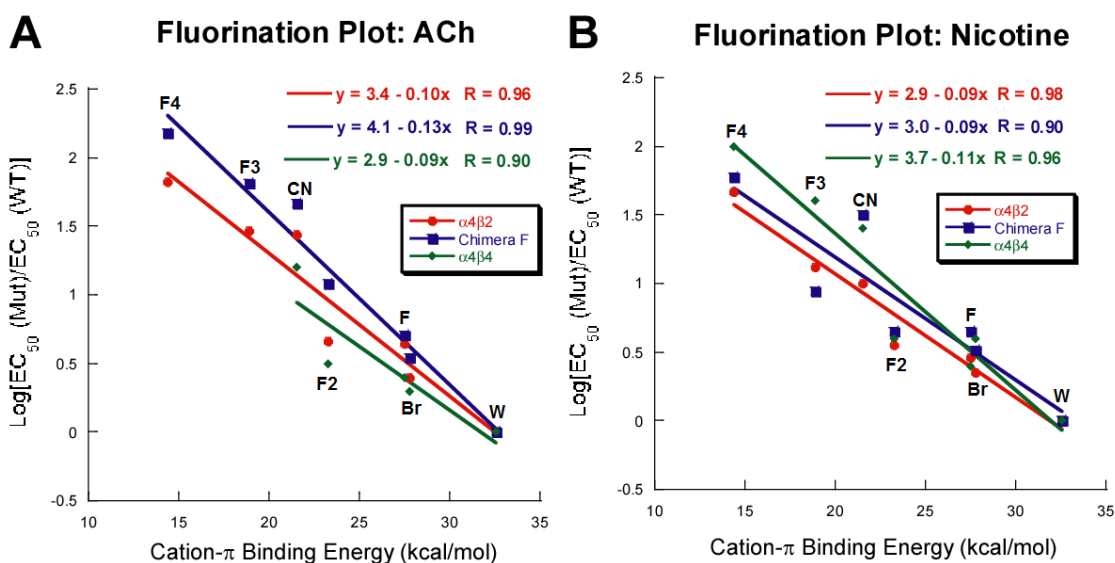


**Figure 4.8.** Cation- $\pi$  binding (fluorination) plots monitor the relative strength of a cation- $\pi$  interaction at TrpB. Data are from Table 4.4. Chimera F (blue) is compared to  $\alpha 4\beta 2$  (red) and  $\alpha 4\beta 4$  (green) for ACh (A) and nicotine (B).

Compared to both  $\alpha 4\beta 2$  and  $\alpha 4\beta 4$ , chimera F strengthened the cation- $\pi$  interaction between ACh and TrpB of the receptor. This was indicated by an increase in

sensitivity to progressive fluorination of TrpB illustrated in the cation- $\pi$  binding plot (**Figure 4.8A**). Nicotine, however, displayed a more variable effect (**Figure 4.8B**). Some mutations displayed an increase in sensitivity to fluorination of TrpB, while others showed a decrease in sensitivity (**Table 4.5**). As such, no significant trend was observed.

**Table 4.5.** Ratios of mutant EC<sub>50</sub> to wild type EC<sub>50</sub>, such that ratios >1 represent loss-of-function. Chimera F (blue) is compared to  $\alpha 4\beta 2$  (red) and  $\alpha 4\beta 4$  (green) for ACh and nicotine. \*Previously reported in Xiu 2009.<sup>2</sup> \*\*Previously reported in Puskar 2011.<sup>1</sup> All other values in this table were determined in the present work. NR = not response.

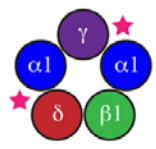
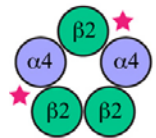
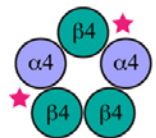
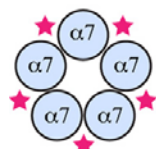
Mutation	Ratio of EC <sub>50</sub> (mutant)/EC <sub>50</sub> (wild type recovery)					
	ACh			Nicotine		
	$\alpha 4\beta 2$ *	Chimera F	$\alpha 4\beta 4$ **	$\alpha 4\beta 2$ *	Chimera F	$\alpha 4\beta 4$ **
Trp	1.0	1.0	1.0	1.0	1.0	1.0
F <sub>1</sub> -Trp	4.3	5.1	2.7	2.9	4.5	2.8
F <sub>2</sub> -Trp	4.5	12	3.4	3.6	4.5	4.1
F <sub>3</sub> -Trp	30	65	NR	13	9	36.5
F <sub>4</sub> -Trp	66	150	NR	47	60	95.0
Br-Trp	2.5	3.5	1.9	2.2	3.3	3.6
CN-Trp	27	47	16.9	10	32	23.0

#### 4.4 DISCUSSION

With >20 nAChR subtypes, these neurotransmitter-gated ion channels are essential for proper brain function and provide a wide array of targets for pharmaceutical development.<sup>4, 5</sup> Given the considerable sequence similarity, especially in the region of the agonist binding site, it becomes quite challenging to discern the mechanisms for differential activation of homologous receptors. Our lab uses unnatural amino acid mutagenesis to address such questions. This method enables subtle and systematic modifications that can isolate specific binding interactions and provide qualitative guidance on the relative magnitudes of specific interactions.

Here, we establish the agonist binding mode for the  $\alpha 4\beta 4$  receptor and contrast drug-receptor interactions for four members of the nAChR family: muscle-type,  $\alpha 4\beta 2$ ,  $\alpha 7$ , and  $\alpha 4\beta 4$  (**Figure 4.9**). Note that the side chains within the aromatic box are identical in all the receptors considered: three tyrosines and two tryptophans. Thus, differences among the receptors must result from subtle structural effects.

**Figure 4.9.** Summary of ligand-receptor interactions present for the muscle-type,  $\alpha 4\beta 2$ ,  $\alpha 4\beta 4$ , and  $\alpha 7$  nAChRs. Stars indicate relevant binding site interfaces.

	ACh	nicotine epibatidine	
	Cation- $\pi$	Cation- $\pi$	H-bond
	TrpB	none TrpB	weak weak
	TrpB	TrpB	strong
	TrpB	TrpB	strong
	TyrA	TyrC2 TyrA	weak

Considering the  $\alpha 4\beta 4$  receptor, the binding of ACh is similar to what has been previously observed for the muscle-type and  $\alpha 4\beta 2$  receptors, but not  $\alpha 7$ . The quaternary ammonium ion of ACh makes a cation- $\pi$  interaction to the face of the aromatic residue TrpB, providing an unambiguous anchor point for ACh docking. The slopes of the cation- $\pi$  binding plots are as follows: 0.095, 0.10, and 0.095 for the  $\alpha 4\beta 4$ ,  $\alpha 4\beta 2$ , and muscle-type nAChRs, respectively.<sup>2, 3</sup> We interpret such similarity in slopes to indicate that the three receptors participate in equally strong cation- $\pi$  interactions between ACh and TrpB. Further, we find that the roles of the other residues of the aromatic box (TyrA, TyrC1, and TyrC2) are similar to those seen in the muscle-type and  $\alpha 4\beta 2$  receptors when

binding ACh. Results for  $\alpha 4\beta 4$  are strikingly different from the  $\alpha 7$  receptor, which uses agonist specific cation- $\pi$  interactions at TyrA and TyrC2.

An interesting result is observed when nicotine is the agonist; now the neuronal  $\alpha 4\beta 4$  receptor acts similarly to the  $\alpha 4\beta 2$  receptor rather than to the muscle-type receptor. In  $\alpha 4\beta 4$ , nicotine makes the same cation- $\pi$  interaction to TrpB as ACh, consistent with the long-accepted nicotinic pharmacophore, but an interaction that is absent in the muscle-type receptor. Interestingly, the slope of the cation- $\pi$  binding plot for  $\alpha 4\beta 4$  is 0.11, which could suggest a moderately stronger cation- $\pi$  interaction at this position than observed for  $\alpha 4\beta 2$  (slope = 0.089).<sup>2</sup> Thus, a cation- $\pi$  interaction to TrpB serves as a discriminator between receptors with higher sensitivity to nicotine ( $\alpha 4\beta 4$  and  $\alpha 4\beta 2$ ) and those with lower sensitivity (muscle-type).

Concerning the hydrogen bond to the backbone carbonyl associated with TrpB,  $\alpha 4\beta 4$  also behaves like  $\alpha 4\beta 2$ , not muscle-type or  $\alpha 7$ . At  $\alpha 4\beta 4$ , nicotine displays a 14-fold decrease in receptor function in response to the backbone ester mutation, comparable to 19-fold for  $\alpha 4\beta 2$ .<sup>2</sup> This contrasts the 1.6-fold shift for muscle-type or 2.1-fold shift for epibatidine at  $\alpha 7$ .<sup>1, 17</sup> Note that when the agonist is ACh – a molecule unable to make a conventional hydrogen bond to a carbonyl – essentially wild type receptor behavior is observed. This indicates that the backbone mutation did not alter receptor function downstream from binding, *i.e.*, gating. We conclude that nicotine is able to make a hydrogen bond to the carbonyl in question in all three receptors considered, but that the interaction is much stronger in  $\alpha 4\beta 4$  and  $\alpha 4\beta 2$ . This is an additional contributor to the enhanced potency of nicotine at the neuronal  $\alpha 4\beta 4$  and  $\alpha 4\beta 2$  receptors. Previous studies

of neuronal nAChRs have indicated that large differences in agonist affinity are primarily determined by the nature of the complementary subunit.<sup>31</sup> Our results provide a molecular rationale indicating that both  $\alpha 4$ -containing neuronal receptors make the same ligand-receptor interactions, but the magnitudes of the two interactions examined differ depending on the receptor, reflecting the nature of the  $\beta$  subunit. For nicotine, the cation- $\pi$  interaction is stronger in the  $\alpha 4\beta 4$  receptor, whereas the hydrogen bond interaction is stronger in the  $\alpha 4\beta 2$  nAChR.

Chimeric  $\beta$  subunits were used to further examine the role of the complementary binding site in defining subtype-specific receptor pharmacology. Using the cation- $\pi$  interaction at TrpB as a probe for agonist binding, we found that most chimeras experienced a modest increase in the  $F_3$ -Trp/Trp ratio compared to  $\alpha 4\beta 2$  and  $\alpha 4\beta 4$ . One exception, however, was nicotine at chimera F, which showed a decreased  $F_3$ -Trp/Trp ratio compared to  $\alpha 4\beta 2$ . Further analysis revealed that chimera F experienced a variable effect in response to additional tryptophan derivatives, and no significant trend was observed. Given that the core residues of the principal binding site are conserved in all nAChRs and chimera studies of the complementary binding site appear less informative, the question remains as to what features of the nAChR are responsible for differences in receptor pharmacology. It is possible that the variable residues flanking the conserved core residues may be the key to understanding the pharmacological diversity of nAChRs. Further experiments are underway to probe both the non- $\alpha$  subunits and residues within the  $\alpha$  subunit that are located outside the aromatic box (Chapter 3).

Here we identify structural features of the nAChR that discriminate among these four receptors and are likely to contribute to differential receptor pharmacology. In the

muscle-type receptor, TrpB makes a cation- $\pi$  interaction to ACh and to epibatidine, but not to nicotine.<sup>3, 16, 17</sup> In the neuronal  $\alpha 4\beta 4$  and  $\alpha 4\beta 2$  receptors, the TrpB cation- $\pi$  interaction to ACh remains, but now nicotine also makes a strong cation- $\pi$  interaction.<sup>2</sup> The  $\alpha 7$  receptor eschews the cation- $\pi$  interaction to TrpB, as agonists have moved their cationic center across the aromatic box to TyrA and TyrC2.<sup>1</sup> The nAChR family also uses a backbone hydrogen bonding interaction as a second discriminating feature for drug-receptor interactions. This interaction is modest in the muscle-type and  $\alpha 7$  receptors,<sup>1, 17</sup> but it is much stronger in  $\alpha 4\beta 4$  and  $\alpha 4\beta 2$ <sup>2</sup> – the higher sensitivity receptors. Taken as a whole, the data support the view that the energy of the cation- $\pi$  and hydrogen bond interactions studied here underlies the higher sensitivity of both  $\alpha 4\beta 2$  and  $\alpha 4\beta 4$ .

## 4.5 METHODS

### *Molecular Biology*

For ligand binding studies of the  $\alpha 4\beta 4$  nAChR (Part 1), human  $\alpha 4$  and  $\beta 4$  subunit genes were in pGEMhe. For chimera experiments (Part 2), rat  $\alpha 4$  and  $\beta 2$  nAChR subunit genes were in the pAMV vector, and as such, chimeras replaced loop regions of the rat  $\beta 2$  subunit with the corresponding regions of the rat  $\beta 4$  subunit. In accordance with previously reported protocols,<sup>2</sup> all  $\alpha 4\beta 2/\beta 4$  chimeric receptors contained a L9'A mutation in the  $\alpha 4$  subunit to increase receptor expression. Site-directed mutagenesis was performed using the QuikChange protocol (Stratagene). For nonsense suppression experiments, the site of interest within the nAChR subunit was mutated to an amber stop codon. Circular DNA for nAChR subunit genes in pAMV were linearized with Not I and nAChR subunit genes in pGEMhe were linearized with Nhe I. After purification

(Qiagen), linearized DNA was used as a template for runoff *in vitro* transcription using T7 mMessage mMachine kit (Ambion).

THG73<sup>32</sup> was used as the amber suppressor tRNA. Nitroveratryloxycarbonyl (NVOC) protected cyanomethyl ester form of unnatural amino acids and  $\alpha$ -hydroxythreonine cyanomethyl ester were synthesized, coupled to dinucleotide dCA, and enzymatically ligated to 74-nucleotide THG73 tRNA<sub>CUA</sub> as previously reported.<sup>20</sup> Crude tRNA-amino acid product was used without desalting, and the product was confirmed by MALDI-TOF MS on 3-hydroxypicolinic acid (3-HPA) matrix. Deprotection of the NVOC group on the tRNA-amino acid was carried out by photolysis for 5 minutes prior to coinjection with mRNA containing the UAG mutation at the site of interest.

### ***Microinjection***

Stage V-VI *Xenopus laevis* oocytes were employed. For experiments in Part 1, coinjection of  $\alpha 4$ : $\beta 4$  mRNA at a ratio of 1:1 by mass or lower yielded wild type ( $\alpha 4$ )<sub>2</sub>( $\beta 4$ )<sub>3</sub> receptors, while a ratio greater than 30:1 by mass produced pure populations of ( $\alpha 4$ )<sub>3</sub>( $\beta 4$ )<sub>2</sub>. If an unnatural amino acid was to be incorporated into the  $\alpha 4$  subunit to produce a ( $\alpha 4$ )<sub>2</sub>( $\beta 4$ )<sub>3</sub> receptor, then a mass ratio of 2:1 for  $\alpha 4$ : $\beta 4$  mRNA was injected into each oocyte.

In Part 2,  $\alpha 4\beta 2/\beta 4$  chimeric receptors were expressed using a co injection of  $\alpha 4$ : $\beta 2/\beta 4$  chimera mRNA at a ratio of 1:3 by mass. This ratio consistently produced chimeric receptors with the stoichiometry of ( $\alpha 4$ )<sub>2</sub>( $\beta 2/\beta 4$ )<sub>3</sub>. For nonsense suppression experiments incorporating an unnatural amino acid into the  $\alpha 4$  subunit, a mass ratio of 3:1 for  $\alpha 4$ : $\beta 2/\beta 4$  chimera mRNA was injected into each oocyte to produce ( $\alpha 4$ )<sub>2</sub>( $\beta 2/\beta 4$ )<sub>3</sub>

receptors. To ensure  $(\alpha 4)_2(\beta 2/\beta 4)_3$  stoichiometry, all receptor stoichiometries were confirmed by voltage jump experiments.<sup>2</sup>

For all experiments (Part 1 and 2), the total mRNA injected was 25-65 ng/oocyte depending on the relative expression level, and approximately 15 ng of tRNA per cell was used for suppression experiments. Each oocyte was injected with 50 nL of RNA solution, and the oocytes were incubated for 24-48 hours at 18 °C in ND96 buffer (96 mM NaCl, 2 mM KCl, 1 mM MgCl<sub>2</sub>, 1.8 mM CaCl<sub>2</sub>, and 5 mM HEPES, pH 7.5) with 0.005% (w/v) gentamycin and 2% (v/v) horse serum. In the case of low-expressing mutant receptors, a second injection was required 24 hours after the first injection. As a negative control for all suppression experiments, 76-nucleotide tRNA (dCA ligated to 74-nucleotide tRNA) was coinjected with mRNA in the same manner as fully charged tRNA.

### ***Electrophysiology***

Acetylcholine chloride and (-)-nicotine tartrate were purchased from Sigma/Aldrich/RBI (St. Louis, MO) and drug dilutions were prepared from 1M *aq* stock solutions. Drug dilutions were prepared in calcium-free ND96 buffer. Ion channel function was assayed using the OpusXpress 6000A (Molecular Devices Axon Instruments) in two-electrode voltage clamp mode. Oocytes were clamped at a holding potential of -60 mV. One mL of each drug solution was applied to the clamped oocytes for 12 sec and followed by a 2 minute wash with calcium-free ND96 buffer between each concentration. Data were sampled at 125 Hz and filtered at 50 Hz. Voltage jump experiments were sampled at 5000 Hz and filtered at 180 Hz.

### ***Data Analysis***

Dose-response data were obtained for at least 6 concentrations of agonists and for a minimum of 5 oocytes (from two different batches). Mutants with  $I_{\max}$  of at least 100 nA of current were defined as functional.  $EC_{50}$  and Hill coefficient ( $n_H$ ) were calculated by fitting the averaged, normalized dose-response relation to the Hill equation. All data are reported as means  $\pm$ S.E.

### **4.6 ACKNOWLEDGEMENTS**

We thank Ariele P. Hanek helpful discussions. This work was supported, in whole or in part, by National Institutes of Health Grants NS34407 and NS11756 and by Grant MH086383 (to H. A. L.). This work was also supported by California Tobacco-Related Disease Research Program Grant 19XT-0102 from the University of California (to D. A. D.).

## 4.7 REFERENCES

1. Puskar, N. L.; Xiu, X.; Lester, H. A.; Dougherty, D. A., Two neuronal nicotinic acetylcholine receptors,  $\alpha 4\beta 4$  and  $\alpha 7$ , show differential agonist binding modes. *J Biol Chem* **286**, (16), 14618-27.
2. Xiu, X.; Puskar, N. L.; Shanata, J. A.; Lester, H. A.; Dougherty, D. A., Nicotine binding to brain receptors requires a strong cation- $\pi$  interaction. *Nature* **2009**, *458*, (7237), 534-7.
3. Zhong, W.; Gallivan, J. P.; Zhang, Y.; Li, L.; Lester, H. A.; Dougherty, D. A., From ab initio quantum mechanics to molecular neurobiology: a cation- $\pi$  binding site in the nicotinic receptor. *Proc Natl Acad Sci U S A* **1998**, *95*, (21), 12088-93.
4. Corringer, P. J.; Le Novere, N.; Changeux, J. P., Nicotinic receptors at the amino acid level. *Annu Rev Pharmacol Toxicol* **2000**, *40*, 431-58.
5. Jensen, A. A.; Frolund, B.; Liljefors, T.; Krosgaard-Larsen, P., Neuronal nicotinic acetylcholine receptors: structural revelations, target identifications, and therapeutic inspirations. *J Med Chem* **2005**, *48*, (15), 4705-45.
6. Romanelli, M. N.; Gratteri, P.; Guandalini, L.; Martini, E.; Bonaccini, C.; Gualtieri, F., Central nicotinic receptors: structure, function, ligands, and therapeutic potential. *ChemMedChem* **2007**, *2*, (6), 746-67.
7. Unwin, N., Refined structure of the nicotinic acetylcholine receptor at 4Å resolution. *J Mol Biol* **2005**, *346*, (4), 967-89.
8. Miyazawa, A.; Fujiyoshi, Y.; Unwin, N., Structure and gating mechanism of the acetylcholine receptor pore. *Nature* **2003**, *423*, (6943), 949-55.
9. Brejc, K.; van Dijk, W. J.; Klaassen, R. V.; Schuurmans, M.; van Der Oost, J.; Smit, A. B.; Sixma, T. K., Crystal structure of an ACh-binding protein reveals the ligand-binding domain of nicotinic receptors. *Nature* **2001**, *411*, (6835), 269-76.
10. Gotti, C.; Clementi, F., Neuronal nicotinic receptors: From structure to pathology. *Prog Neurobiol* **2004**, *74*, (6), 363-96.
11. Romanelli, M. N.; Gratteri, P.; Guandalini, L.; Martini, E.; Bonaccini, C.; Gualtieri, F., Central Nicotinic Receptors: Structure, Function, Ligands, and Therapeutic Potential. *ChemMedChem* **2007**, *2*, (6), 746-767.
12. Beers, W. H.; Reich, E., Structure and activity of acetylcholine. *Nature* **1970**, *228*, (5275), 917-22.
13. Glennon, R. A.; Dukat, M., Central nicotinic receptor ligands and pharmacophores. *Pharm Acta Helv* **2000**, *74*, (2-3), 103-14.
14. Sixma, T. K.; Smit, A. B., Acetylcholine binding protein (AChBP): a secreted glial protein that provides a high-resolution model for the extracellular domain of pentameric ligand-gated ion channels. *Annu Rev Biophys Biomol Struct* **2003**, *32*, 311-34.
15. Blum, A. P.; Lester, H. A.; Dougherty, D. A., Inaugural article: Nicotinic pharmacophore: the pyridine N of nicotine and carbonyl of acetylcholine hydrogen bond across a subunit interface to a backbone NH. *Proc Natl Acad Sci U S A* **107**, (30), 13206-11.
16. Beene, D. L.; Brandt, G. S.; Zhong, W.; Zacharias, N. M.; Lester, H. A.; Dougherty, D. A., Cation- $\pi$  interactions in ligand recognition by serotonergic (5-

- HT3A) and nicotinic acetylcholine receptors: the anomalous binding properties of nicotine. *Biochemistry* **2002**, 41, (32), 10262-9.
17. Cashin, A. L.; Petersson, E. J.; Lester, H. A.; Dougherty, D. A., Using physical chemistry to differentiate nicotinic from cholinergic agonists at the nicotinic acetylcholine receptor. *J Am Chem Soc* **2005**, 127, (1), 350-6.
  18. Xiu, J. Structure-Function Studies of Nicotinic Acetylcholine Receptors Using Unnatural Amino Acids. The California Institute of Technology, Ph.D. Thesis, Pasadena, 2007.
  19. Wu, J.; Liu, Q.; Yu, K.; Hu, J.; Kuo, Y. P.; Segerberg, M.; St John, P. A.; Lukas, R. J., Roles of nicotinic acetylcholine receptor beta subunits in function of human alpha4-containing nicotinic receptors. *J Physiol* **2006**, 576, (Pt 1), 103-18.
  20. Nowak, M. W.; Gallivan, J. P.; Silverman, S. K.; Labarca, C. G.; Dougherty, D. A.; Lester, H. A., In vivo incorporation of unnatural amino acids into ion channels in *Xenopus* oocyte expression system. *Methods Enzymol* **1998**, 293, 504-29.
  21. Padgett, C. L.; Hanek, A. P.; Lester, H. A.; Dougherty, D. A.; Lummis, S. C., Unnatural amino acid mutagenesis of the GABA(A) receptor binding site residues reveals a novel cation-pi interaction between GABA and beta 2Tyr97. *J Neurosci* **2007**, 27, (4), 886-92.
  22. Lummis, S. C.; D, L. B.; Harrison, N. J.; Lester, H. A.; Dougherty, D. A., A cation-pi binding interaction with a tyrosine in the binding site of the GABAC receptor. *Chem Biol* **2005**, 12, (9), 993-7.
  23. Mu, T. W.; Lester, H. A.; Dougherty, D. A., Different binding orientations for the same agonist at homologous receptors: a lock and key or a simple wedge? *J Am Chem Soc* **2003**, 125, (23), 6850-1.
  24. Torrice, M. M.; Bower, K. S.; Lester, H. A.; Dougherty, D. A., Probing the role of the cation-pi interaction in the binding sites of GPCRs using unnatural amino acids. *Proc Natl Acad Sci U S A* **2009**, 106, (29), 11919-24.
  25. Moroni, M.; Zwart, R.; Sher, E.; Cassels, B. K.; Bermudez, I., alpha4beta2 nicotinic receptors with high and low acetylcholine sensitivity: pharmacology, stoichiometry, and sensitivity to long-term exposure to nicotine. *Mol Pharmacol* **2006**, 70, (2), 755-68.
  26. Nelson, M. E.; Kuryatov, A.; Choi, C. H.; Zhou, Y.; Lindstrom, J., Alternate stoichiometries of alpha4beta2 nicotinic acetylcholine receptors. *Mol Pharmacol* **2003**, 63, (2), 332-41.
  27. Nowak, M. W.; Kearney, P. C.; Sampson, J. R.; Saks, M. E.; Labarca, C. G.; Silverman, S. K.; Zhong, W.; Thorson, J.; Abelson, J. N.; Davidson, N.; et al., Nicotinic receptor binding site probed with unnatural amino acid incorporation in intact cells. *Science* **1995**, 268, (5209), 439-42.
  28. Espinoza-Fonseca, L. M.; Trujillo-Ferrara, J. G., Fully flexible docking models of the complex between alpha7 nicotinic receptor and a potent heptapeptide inhibitor of the beta-amyloid peptide binding. *Bioorg Med Chem Lett* **2006**, 16, (13), 3519-23.
  29. Hussy, N.; Ballivet, M.; Bertrand, D., Agonist and antagonist effects of nicotine on chick neuronal nicotinic receptors are defined by alpha and beta subunits. *J Neurophysiol* **1994**, 72, (3), 1317-26.

30. Luetje, C. W.; Patrick, J., Both alpha- and beta-subunits contribute to the agonist sensitivity of neuronal nicotinic acetylcholine receptors. *J Neurosci* **1991**, 11, (3), 837-45.
31. Parker, M. J.; Beck, A.; Luetje, C. W., Neuronal nicotinic receptor beta2 and beta4 subunits confer large differences in agonist binding affinity. *Mol Pharmacol* **1998**, 54, (6), 1132-9.
32. Saks, M. E.; Sampson, J. R.; Nowak, M. W.; Kearney, P. C.; Du, F.; Abelson, J. N.; Lester, H. A.; Dougherty, D. A., An engineered Tetrahymena tRNA<sup>Gln</sup> for in vivo incorporation of unnatural amino acids into proteins by nonsense suppression. *J Biol Chem* **1996**, 271, (38), 23169-75.